Study of Muon Neutrino Oscillations Using MicroBooNE Data

Third Year Lab Report

Herbie Warner
10829700
Department of Physics and Astronomy, University of Manchester
(Experiment performed in collaboration with Ian Osborne)

(Dated: December 15, 2023)

This work presents a method for minimising the likelihood of presented eV-scale sterile neutrino oscillations from the LSND, and MiniBooNE detectors by using MicroBooNE data. Such minimisation is installed via a Neuroevolutionary network, of a coupled Genetic Algorithm, and Convolutional Neural Network, that make selection cuts to Monte-Carlo data from the GENIE neutrino event generator. A simplified error framework is assumed, along with singular oscillation. The implementation derives contours at the 95% confidence level in the plane of the mass-squared splitting Δm^2_{41}, and the sterile neutrino mixing angle $\theta_{\mu e}$, finding exclusion of 50% of the parameter space allowed by experimental anomalies in the LSND data. However, a Pareto efficiency is found between the purity, efficiency, and exclusion region, indicating this is not a viable method for resolving the LSND and MiniBooNE anomalies.

1. INTRODUCTION

The resolution of the Solar Neutrino Problem [1, 2] has given rise to a large scientific enquiry into the study of neutrino oscillations, with most of such research consistent with the three flavour framework described by the PontecorvoMaki-Nakagawa-Sakata (PMNS) formalism [3]. Several experimental anomalies [4] find resolution in a hypothetical sterile neutrino: an additional fourth neutrino flavour with a mass in the eV-scale. The MicroBooNE detector, a liquid argon Time Projection Chamber [5], seeks to provide further insight into such anomalies. By oscillating Monte-Carlo data (MC) under the 3 + 1 active-to-sterile neutrino oscillation framework, and comparing to MicroBooNE data, the confidence levels (CL) of different regions of parameter space can be evaluated: parameter space is the plane of the mass-squared splitting Δm^2_{41}, and the sterile neutrino (ν_s) mixing angle $\theta_{\mu e}$. The chi squared analysis will indicate to what confidence the MiniBooNE and LSND anomalies are resolved by the inception of a ν_s. This is only valid in the case of pure data, and as such selection cuts are designed to maximise purity.

2. THEORY

Oscillation to a fourth flavour requires the use of an extended 4×4 unitary PMNS matrix (U) [3], to relate the mass and flavour eigenstates. Assuming $\Delta m^2_{41} \gg \Delta m^2_{31}$ the probability of oscillation between flavour- α and flavour-β, under U, is approximately given by

$$P(\alpha \to \beta) = \delta_{\alpha\beta} + (-1)^{\delta_{\alpha\beta}} \sin^2(2\theta_{\alpha\beta}) \sin^2(\frac{\Delta m^2_{41} L}{4E}), \tag{1}$$

where $\delta_{\alpha\beta}$ is the Kronicker Delta, L is the distance from the source, E is the energy of the neutrino, and $\theta_{\alpha\beta}$ is the mixing angle between flavours α and β. This analysis only applies ν_μ disappearance, and thus the only oscillation of interest is

$$P(\nu_\mu \to \nu_e) = \sin^2(\theta_{24}) \sin^2(2\theta_{14}) \sin^2(1.27\frac{\Delta m^2_{41} L}{E}), \tag{2}$$

with the 1.27 arising from a unit conversion. This formula is applied to the MC data across parameter space to evaluate which regions give the lowest χ^2, and comparing to those regions produced by LSND and MiniBooNE.

3. METHOD

To exclude regions of parameter space the data, both the real from MicroBooNE Run 3 [3], and the MC from the GENIE neutrino event generator [6], is filtered with selection cuts. These aim to remove noise without removing significant quantities of signal events. The quality of a cut is gauged by the purity,

$$P = \frac{\text{Number of remaining signal events}}{\text{Total number of remaining events}}, \tag{3}$$

and the efficiency,

$$\textit{Eff} = \frac{\text{Events surviving the selections}}{\text{Original number of events}}. \tag{4}$$

Assuming the MC data is suitably generated and adapted, it is arguable that a high purity on the MC, which is exactly calculable, implies a high purity on the real data as well. Improper generation/adaption will undermine P calculations, invalidating any conclusion drawn. This will also instill biases in features trained on the MC, such as Topological Score, rendering cuts on that feature unjustifiable. The MC data is assumed well adapted in this analysis. It is however possible to obtain errors on P by using methods such as decision trees to identify particle type in the real data, but this is not implemented in this analysis.

The features that can be cut are shown in Table I. The Track Score quantifies how much a signal resembles a track, and the Topological Score quantifies how much said track looks like a ν_μ. The Track Momentum is the particle momentum determined via multiple Coulomb scattering, and the Track Distance is the distance between the track and a reconstructed neutrino vertex. The Track Length is the distance between the start and end of a track.

3.1. Genetic Algorithm

A Genetic Algorithm (GA) is a meta heuristic inspired by natural selection [7]. The purpose of the GA here is to find a selection cut that maximises the purity, whilst retaining a sufficient efficiency. The nomenclature for attributes in this particular implementation are as follows.

An individual is a unique set of selection cuts, with each cut to a particular feature named a gene. An example of an individual is given in Table I. Also associated with each individual is a metric of its performance: the P and *Eff*.

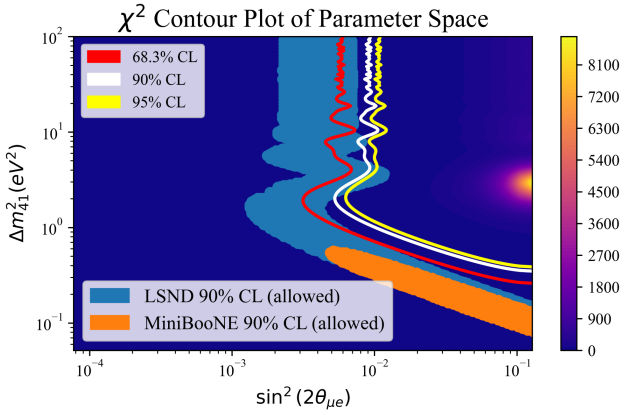

FIG. 1. Best individual after 50 generations of the GA. Metrics: $P = 96\%, Eff = 11\%$. LSND and MiniBooNE show the 90% CL allowed regions within the 3 + 1 framework.

The population consists of many of these individuals such that enough genetic diversity is seeded to insure wide exploration of feature space: feature space is spanned by the features in Table I with extension to the *P-Eff* space. After calculating the metrics the best individuals are installed into the next generation. Others crossover which mix their genes to produce offspring that are then seeded into the new population; some genes are randomly mutated to encourage further exploration and prevent premature local convergence. This process repeats up to a certain number of generations, or the metric surpasses some threshold.
Figure 1 shows the best individual after 50 generations of the GA. The 96% purity indicates a high likelihood that the real data represents ν_μ oscillation, significantly enhancing the reliability and accuracy of conclusions drawn. However the MiniBooNE region is not excluded at any measured CL, counter to the MicroBooNE findings [3]. This indicates a high purity does not necessarily imply region exclusion, and thereby motivates the introduction of a new metric for the exclusion itself.

3.2. *Hybrid Network*

Analysis reveals it is not possible to discern where the CLs rest in parameter space from these two metrics alone: the *P-Eff* space is degenerate. A third metric is thusly introduced called the χ^2_m. This is calculated as the average horizontal relative index difference of an LSND data point, and the 95% CL. Figure 1 has a $\chi^2_m = 0.15$.
The minimisation of the χ^2_m can be achieved by slight alteration of the GA. However the exact calculation of the χ^2_m is computationally intensive taking around thirty seconds per individual, which, extrapolated to the population, yields a considerable increase in run time. One solution is integrating a CNN, trained on individuals to output their metrics, into the GA to create a neuroevolutionary hybrid network. This implementation not only quickens calculations, but also provides other optimisation enhancements.
To install effective convolution, and thus reliable predictions from the CNN, the individuals are now represented by matrices consisting of cycled density-weighted binary arrays. Each array corresponds to a different feature, with the binary elements in each encoding whether to pass data in that bin. These elements are weighted by the number of data points in that bin, thereby assigning more importance to those bins with higher event counts. The arrays are also cyclically rotated such that each row has better column overlap with one another, mitigating the inter-row column dependence - useful patterns may exist beyond adjacent elements in adjacent rows. Non-Euclidean convolutions can also be applied to cover row-to-row dependence, allowing pattern identification between cuts to all features, and not just the ones adjacent in the matrix. This representation better encapsulates the spatial information manifest in the cuts, compared to the direct parsing as floats.

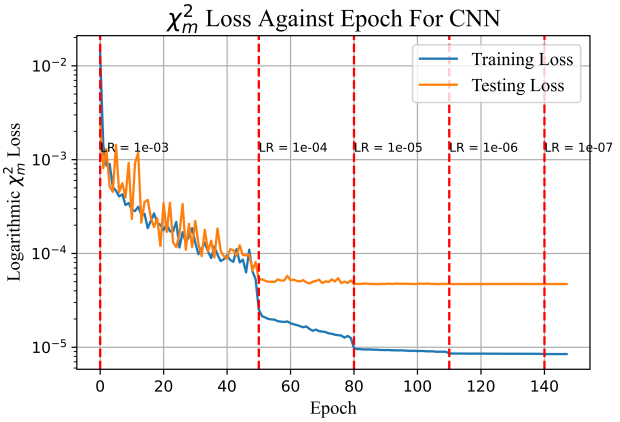

FIG. 2. Logarithmic mean squared error for predicting the χ^2_m for an individual. LR is the adaptive learning rate. Minimum validation loss: 4.72×10^{-5}.

Figure 2 shows the loss against epoch for training the CNN. Weights are restored to produce the lowest validation loss to prevent overfitting. The validation loss indicates on average

$$\chi^2_{m^{\text{true}}} = \chi^2_{m^{\text{predict}}} \pm 0.007, \tag{5}$$

where $\chi^2_{m^{\text{true}}}$ is the exactly calculated χ^2_m for an individual, and $\chi^2_{m^{\text{predict}}}$ is the CNNs prediction. The domain of this metric is $-1 \leq \chi^2_m \leq 1$ indicating good reliability.

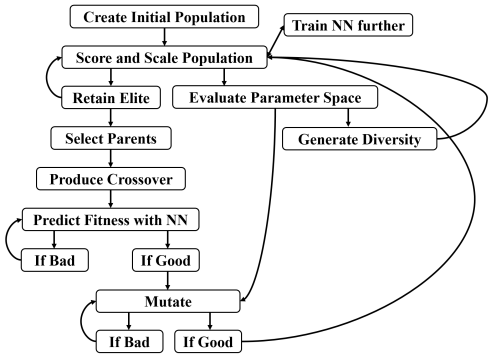

FIG. 3. Flow chart of hybrid network.

.

Figure 3 shows full the hybrid network procedure. Now bad genes propagated by random mutations and crossovers can be pruned by predicting the new individuals metrics, and repeating if such metrics are worse than their predecessors. Further enhancements are made by evaluating feature space, steering the evolution of solutions away from undesirable genetics, and towards those more promising; exhaustive exploration also encourages genetic diversity by the insertion of genes not currently manifest in the population, increasing the likelihood of a global convergence.

4. RESULTS AND ANALYSIS

The best individual is shown in Table I and the corresponding χ^2 contour plot in Figure 4. The data at the lowest χ^2

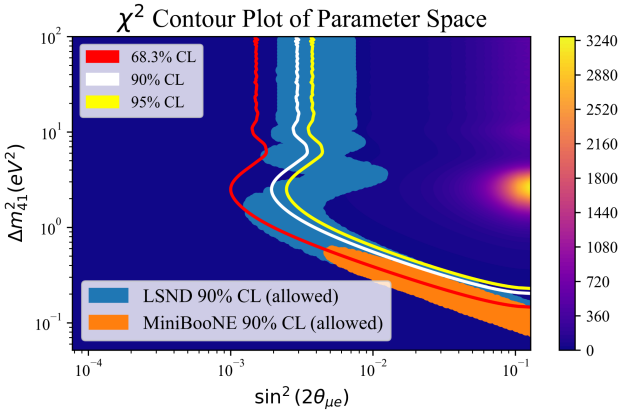

FIG. 4. Best individual after 50 generations of hybrid network. Metrics: $\chi^2_m = -0.0009, P = 83\%, Eff = 14\%$. LSND and MiniBooNE show the 90% CL allowed regions within the 3 + 1 framework.

Feature	Values
Topological Score	(0.059, 0.062), (0.128, 0.140), (0.192, 0.221), (0.277, 0.305), (0.354, 0.354), (0.368, 0.460), (0.472, 0.504), (0.524, 0.530), (0.576, 0.594), (0.623, 0.639), (0.655, 0.683), (0.730, 0.731), (0.770, 0.830), (0.836, 0.884), (0.946, 0.955)
Track Length	(0.6, 40), (50, 650)
Track Distance	(0.0, 8)
Track Score	(0.8, 1)
Track Muon Momentum	(0.2, 1.5)

TABLE I. Best individual from hybrid network. Tuple indicates to pass events with feature value in that domain.

value is shown in Figure 5. Comparison to published results [3] is inappropriate however. The covariance matrices of the detector are not installed, nor the errors from GENIE [6]: these will mitigate additional systematics introduced by possible bias. Furthermore only ν_μ are oscillated. This analysis assumes a flat 15% systematic uncertainty [8], and a Poisson distribution for the statistical.

The χ^2_m is extremely sensitive to fluctuations in the the systematic uncertainty, with the individual in Table I reaching a $\chi^2_m = -0.13$ for a systematic uncertainty of 10%. Resolution requires implementation of the full covariance matrices from MicroBooNE, along with the uncertainties associated with GENIE. To ensure appropriate use of the Poisson distribution, constraints were installed such that no bin can be less than a certain height, except for the low energy bins in which the data is already scarce (Figure 5). This requirement prevents the distribution from being too sparse allowing reliable probabilistic descriptions. The bin widths are 0.1 GeV as per the detector sensitivity [5].

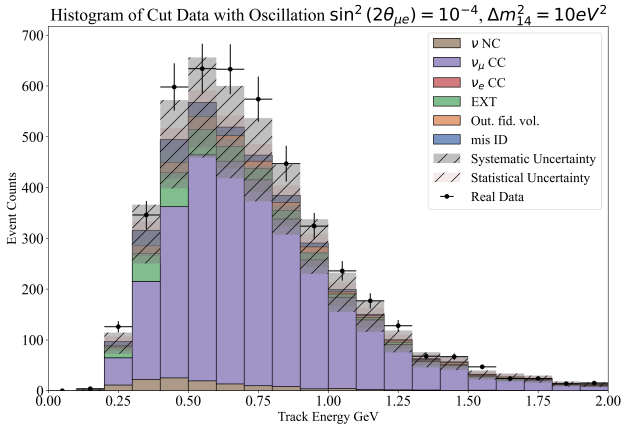

FIG. 5. Histogram showing the data cut with individual in Table I and best oscillation parameters $\sin^2(2\theta_{\mu e}) = 10^{-4}$ and, $\Delta m^2_{14} = 10eV^2$. Reduced $\chi^2 = 1.33$.

Comparison of Figures 4 and 1 indicate that a high purity does not imply a low χ^2_m. There exists a Pareto efficiency between the metrics; the model can not constrain itself to both pure data, and minimising the χ^2_m concurrently. This necessary background retention reduces result confidence thereby inhibiting meaningful conclusions. This method is thus not a viable solution to this particular optimisation problem.

5. CONCLUSION

The optimisation method employed excludes 50% of the parameter space allowed by experimental anomalies seen in the LSND data at the 95% confidence level. Such rejection incurs an efficiency of 14% and a purity of 83%. The network only achieves this assuming the systematics to be a constant 15%, the data to be poisson distributed, and the only neutrino oscillation to be that of the ν_μ. The rectification of these requires use of covariance matrices, a more suitable statistical analysis on a per individual basis, and the inclusion of other oscillations respectively. It is furthermore assumed the MC data is adapted well to the real, and the topological score is not bias to the MC. The network can however produce highly pure data, but results from such run counter to the MicroBooNE findings [3].
The network is nascent, with potential enhancements manifold, such as, dynamic population size, and adaptive mutations. However, with its current form it can not succeed in both region exclusion and maximisation of the purity, and therefore is not a viable approach to exclusion attempts.

[1] B. T. Cleveland *et al.*, The Astrophysical Journal **496**, 505 (1998).
[2] J. Boger *et al.*, Nuclear Instruments and Methods in Physics Research Section A: Accelerators, Spectrometers, Detectors and Associated Equipment **449**, 172 (2000).
[3] P. Abratenko *et al.*, Physical Review Letters **130**, 10.1103/physrevlett.130.011801 (2023).
[4] V. V. Barinov *et al.*, Physical Review C **105**, 10.1103/physrevc.105.065502 (2022).
[5] R. Acciarri *et al.*, Journal of Instrumentation **12** (02), P02017–P02017.
[6] The MicroBooNE Collaboration, *Neutrino Interaction Model and Uncertainties for MicroBooNE Analyses*, Tech. Rep. MICROBOONE-NOTE-1074-PUB (MicroBooNE, 2020).
[7] T. Alam, S. Qamar, A. Dixit, and M. Benaida, CoRR **abs/2007.12673** (2020), 2007.12673.
[8] J. Waiton, Study of Muon Neutrino Oscillations Using MicroBooNE Data (2023), lab script.